Demonstration and origin of six tertiary base pair resonances in the NMR spectrum of E. coli tRNA1Val

Reid, Brian R.; Robillard, George T.

Published in:
Nature

DOI:
10.1038/257287a0

Table 3 Estimated integral external free-air γ doses (rad)

	Time interval (yr) 5	10	30	70
Ia/Unmodified	0.76	1.37	3.12	5.33
1. Village gravelled	(0.62)	(1.12)	(2.58)	(4.51)
2. +Janet ploughed	(0.41)	(0.75)	(1.77)	(3.27)
3. +Northern islands ploughed	(0.30)	(0.56)	(1.40)	(2.76)
Ib/Unmodified	0.83	1.49	3.35	5.65
1. Village gravelled	(0.71)	(1.28)	(2.89)	(4.96)
2. +Janet ploughed	(0.49)	(0.87)	(2.01)	(4.96)
3. +Northern islands ploughed	(0.33)	(0.61)	(1.50)	(2.90)
II/Unmodified	0.38	0.68	1.59	2.97
3. Northern islands ploughed	(0.22)	(0.41)	(1.08)	(2.26)
III/Unmodified	0.60	1.10	2.60	4.60
1. Village gravelled	(0.48)	(0.88)	(2.14)	(3.90)
2. +Janet ploughed	(0.25)	(0.48)	(1.26)	(2.56)
IV/Unmodified	0.14	0.28	0.83	1.92
Mean population dose (average of cases Ib–IV)				
Unmodified	0.49	0.89	2.09	3.79
1. Village gravelled	(0.43)	(0.78)	(1.86)	(3.44)
2. +Janet ploughed	(0.32)	(0.58)	(1.42)	(2.77)
3. +all northern islands ploughed	(0.24)	(0.45)	(1.17)	(2.41)
Sea level USA (80 mrad yr^{-1}) typical	0.40	0.80	2.40	5.60

or turning over the soil rather than mixing it would, of course, result in even greater reductions in exposure rate. For example, mixing to a depth of 60 cm would reduce the exposure rates by an additional factor of 2, whereas covering the sources with approximately 30 cm of uncontaminated soil would essentially reduce the exposure rates to negligible values similar to those observed on the southern islands. Removing the top 15 cm of soil, which often contains about two-thirds of the activity, would result in a threefold reduction in the exposure rates. The advantages of ploughing or removing the topsoil should, however, be considered on a case-by-case basis because of the highly variable distributions of activity with depth.

From Table 3 it can be seen that extensive modifications may not be required to reduce the dose levels to values comparable to typical US values[2]. Keeping in mind that the selected cases represent approximations to the most likely living patterns, one observes that even for cases *Ia* and *Ib*, the unmodified 70-yr integral doses are comparable to the US values, although cases II and IV lead to considerably lower doses. The mean integrated doses shown in Table 3 were derived by averaging those for cases *Ib*, II, III and IV. This implies that half the returning population live on Janet and the other half live on Fred, Elmer or David and that trips to the northern or southern islands are equally likely for both groups. The unmodified mean population doses are all quite comparable with US values. At most, implementation of modifications 1 and 2 should be enough to assure mean population exposures well below the US levels.

Because of the low amount of natural radioactivity normally present in the coral atolls, the external dose levels calculated for cases I–III are still appreciably higher than corresponding levels found elsewhere in the Marshall Islands (essentially case IV). The results for cases II and IV indicate that restricting the permanent villages to 'clean' southern islands at least temporarily would result in lower exposures.

All of the doses discussed so far result from free-air γ-ray plus cosmic-ray exposures. The effect of shielding by structures or the body itself on gonadal or bone doses has been ignored. To convert from free-air dose (rads) to gonadal dose (rem), a body-shielding factor of 0.8 may be used[3].

Received March 5; accepted August 4, 1975.

1 Eniwetok Radiological Survey, US Atomic Energy Commission Report NVO 140, Vol. I–III (Nevada Operations Office, Las Vegas, Nevada, 1973).
2 Beck, H. L., Lowder, W. J., Bennett, B. G., and Condon, W. J., *Further Studies of External Environmental Radiation*, USAEC, Health and Safety Laboratory Report HASL-170, Table IV (1966).
3 *Report of the United Nations Scientific Committee on the Effects of Ionizing Radiation: Levels and Effects*, Vol. 1, Levels, Annex A, 38 (1972).

Demonstration and origin of six tertiary base pair resonances in the NMR spectrum of *E. coli* $tRNA_1^{Val}$

Brian R. Reid
Biochemistry Department, University of California, Riverside, California 92502
George T. Robillard
Department of Physical Chemistry, University of Groningen, Groningen, The Netherlands

The 360-MHz NMR spectrum of E. coli $tRNA_1^{Val}$ *reveals 26 resonances, six of which are derived from tertiary base pairs. The origin of these tertiary resonances and their approximate positions in the spectrum are discussed in relation to the crystal structure of tRNA.*

EACH Watson–Crick base pair generates a single low field nuclear magnetic resonance (NMR) derived from the ring NH hydrogen bond[1]. Kearns *et al.*[2,3] showed that the ring NH hydrogen bonds from base pairs in tRNA in H_2O solutions, although solvent-exchangeable, possessed adequately long helix lifetimes to generate discrete resonances with chemical shifts in the −11 p.p.m. to −15 p.p.m. region. High resolution NMR studies of several class I tRNA species (20±1 cloverleaf base pairs) have been carried out; the spectra were interpreted to contain 20±1 low field resonances from secondary base pairs, that is it was claimed or assumed that no extra resonances from tertiary base pairs were present[2–14].

We recently showed that, of all the class I tRNA species so far studied, *Escherichia coli* $tRNA_1^{Val}$ exhibited the best-resolved low field NMR spectrum; integration of the 270-MHz spectrum of this tRNA on the assumption that several resolved peaks contained a single proton, indicated

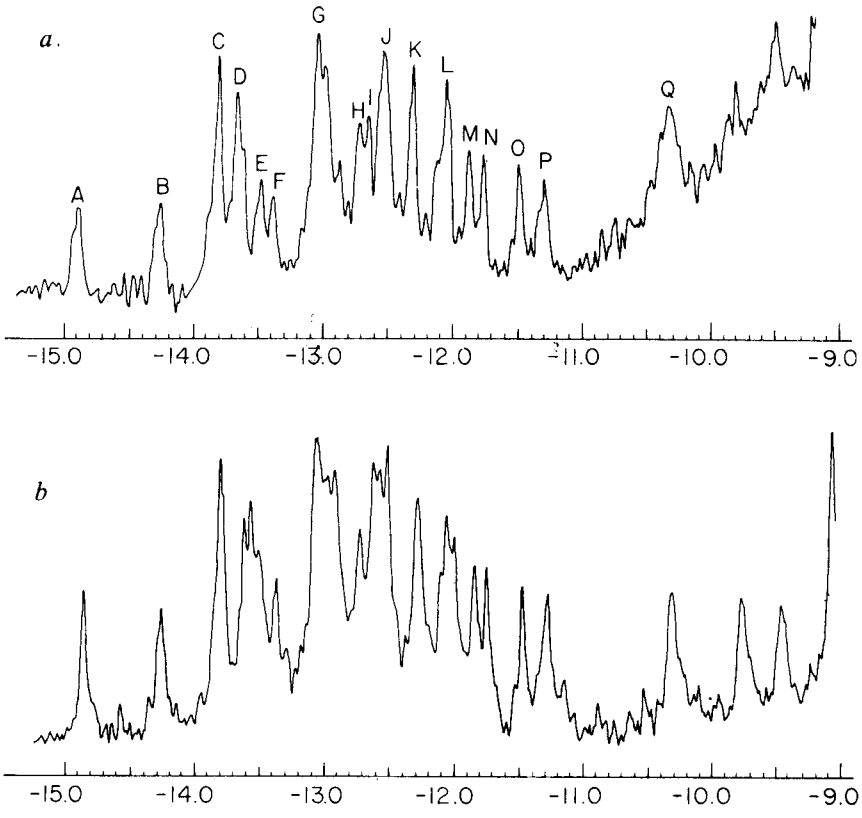

Fig. 1 360-MHz spectrum of *E. coli* $tRNA_1^{Val}$ in the presence (*a*) and absence (*b*) of magnesium. The solvent for the upper spectrum was 10 mM Na cacodylate, 15 mM $MgCl_2$, 0.1 M NaCl, 1 mM EDTA, *p*H 7.0. The solvent for the lower spectrum was 10 mM Na cacodylate, 10 mM EDTA, *p*H 7.0. In both samples the tRNA concentration was approximately 25 mg ml^{-1} (about 1 mM) and the spectra were signal averaged for several hours to improve signal-to-noise ratio.

that, contrary to previous interpretations, the spectrum contained several extra resonances derived from tertiary base pairs[15]. We have now reinvestigated *E. coli* $tRNA_1^{Val}$ at 360 MHz; the improved resolution reveals six tertiary base pairs in the solution structure of this tRNA. The demonstration of 26 ± 1 base pairs is independently corroborated by calibrating the intensity of the low field spectrum with respect to the intensity of the methyl resonances of the three methylated bases in the molecule.

Internal calibration of 360-MHz spectrum

E. coli $tRNA_1^{Val}$ was purified to 98% homogeneity by standard chromatographic procedures. Figure 1 shows the 360-MHz spectrum at 35 °C; in the presence of Mg^{2+} (Mg^{2+}–tRNA ratio of 15) and in the absence of magnesium. In the magnesium-containing spectrum there are 16 resolved peaks between −11 p.p.m. and −15 p.p.m. In our previous spectra at 270 MHz we were able to integrate with respect to the single proton peaks at −14.9 p.p.m. and −14.3 p.p.m. and establish that the total intensity corresponded to 26 ± 3 protons. Now, with the superior resolution at 360 MHz, we can integrate most peaks individually. Peaks A, B, E, F, M, N, O, P have the same intensity which we assume to correspond to one proton. Based on this assumption peaks C, D, K and peak H+I correspond (with an error of less than 10%) to two protons. Peak J contains three protons and peak G contains five protons; peak L corresponds to an intensity significantly greater than two protons. The experimental peak intensities and their nearest integral values are listed in Table 1. Thus integration of resolved individual peaks enables us to determine the overall intensity with much greater accuracy and leads to a value of 26 ± 1 protons. Since there are only 20 secondary base pairs in this tRNA (Fig. 3) this establishes that there are at least six tertiary base pairs involving ring N · · · H bonds in the solution structure.

Table 1 Integrated intensities of individual peaks in the 360 MHz spectrum of *E. coli* $tRNA_1^{Val}$

Peak	Position (p.p.m.)	Intensity	Integral value
A	−14.9	0.8	1
B	−14.3	1.0	1
C	−13.8	2.0	2
D	−13.7	2.1	2
E, F	−13.5, −13.4	1.9	2
G	−13.0	5.0	5
H, I	−12.7, −12.6	2.1	2
J	−12.5	3.0	3
K	−12.3	1.9	2
L	−12.1	2.4	2–3
M	−11.9	1.0	1
N	−11.8	0.9	1
O	−11.5	0.9	1
P	−11.3	0.9	1
		Total	26 ± 1

Independent calibration based on methyl resonance intensity

The validity of the assumption that the resolved small peaks in Fig. 1 contain one proton can be justified on the grounds that, if they contained two protons the spectrum would indicate 54 base pairs which is impossible with only 76 nucleotides. Since the conclusion that six resonances from tertiary base pairs were present in the spectrum is, however, contrary to all previous interpretations of class I tRNA spectra, we felt it was important to calibrate independently the intensity of a single proton.

A sample of 11 mg of *E. coli* $tRNA_1^{Val}$ was dissolved in 2.1 ml of water and two samples of 1.00 ml were lyophilised in separate small tubes. The first sample was dissolved in 0.20 ml of D_2O and the high field spectrum in the methyl region was taken; the second sample was dissolved in 0.20 ml of the normal H_2O buffer and the low field spectrum taken as usual. Both spectra were accumulated

for the same number of sweeps at the same r.f. power. Figure 2 shows the two spectra. There are three resolved peaks of equal intensity at −2.8 p.p.m., −2.6 p.p.m. and −1.1 p.p.m. in the region expected for methyl resonances. Figure 3 shows the cloverleaf structure of *E. coli* $tRNA_1^{Val}$ which contains three methylated bases, namely m^6A37, m^7G46 and rT54. Thus the three methyl peaks in the high field spectrum define the intensity of three protons at the same spectrometer settings used in the low field spectrum. Peaks A, B, M, N, O, P all have an intensity between 30% and 35% of the methyl intensity, thus establishing unequivocally that they are in fact single protons. Furthermore, the overall intensity of the low field spectrum is 8.5 times the methyl resonance intensity, again corroborating the presence of 26 ± 1 base pairs.

Previous assignments of methyl resonances in tRNA by Kan *et al.*[16] enable us to assign the peak at −1.1 p.p.m. to rT54. The peaks at −2.8 p.p.m. and −2.6 p.p.m. must be m^7G46 and m^6A37 and, based on the data of Kan *et al.*[16], the −2.8 p.p.m. peak can be tentatively assigned to m^7G46. The peak at −1.2 p.p.m. has an intensity of approximately 2 protons and is probably the methylene protons of the oxyacetic side chain of residue V34 in the wobble position of the anticodon triplet. The peak at −0.2 p.p.m. is a solvent contaminant, but there is still some rather diffuse intensity between −0.7 p.p.m. and −2.5 p.p.m. which may be derived from hU17.

Base pairs contributing tertiary resonances

The crystal structure of yeast $tRNA^{Phe}$ has been determined at 3 Å resolution[17,18]. The fact that almost all positions involved in tertiary bonding in yeast $tRNA^{Phe}$ are occupied by the same nucleotide in *E. coli* $tRNA_1^{Val}$, together with more detailed arguments on the general structure of class I tRNAs[19,20], prompted us to consider the origin of the tertiary base pair resonances on the basis of the crystallographic data. The five known tertiary interactions involving ring NH hydrogen bonds are shown in Fig. 4. Four of these involve ring NH · · · ring N bonds and one (G15-C48) involves a ring NH which bonds to an exocyclic carbonyl oxygen; hydrogen bonding to carbonyl oxygens is less deshielding and would be expected to generate a ring NH resonance towards the high field end of the −11 to −15 p.p.m. region[1]. There are nine tertiary interactions seen in the crystal structure[17,18]; however, three of them (A9 to AU12; A21 to A14; G26 to A44 or A26 to G44 in $tRNA_1^{Val}$), involve exocyclic amino hydrogen bonds instead of ring NH bonds and thus would not be expected to contribute to the −11 to −15 p.p.m. region of the spectrum[1]. The last tertiary pair is G18–ψ55. The precise bonding in this interaction has not been determined unambiguously; however, recent data (A. Rich, personal communication) indicate that it involves a ring NH proton which probably bonds to a ribose oxygen. Such bonding would lead to a tertiary resonance which would also be expected to be towards the high field end of the −11 to −15 p.p.m. region of the spectrum. The crystallographic data showing five definite and one probable tertiary interaction involving ring NH bonds, and the data presented here showing six tertiary ring NH resonances, are in excellent agreement. Our data are completely consistent with the crystal structure being the actual structure in solution.

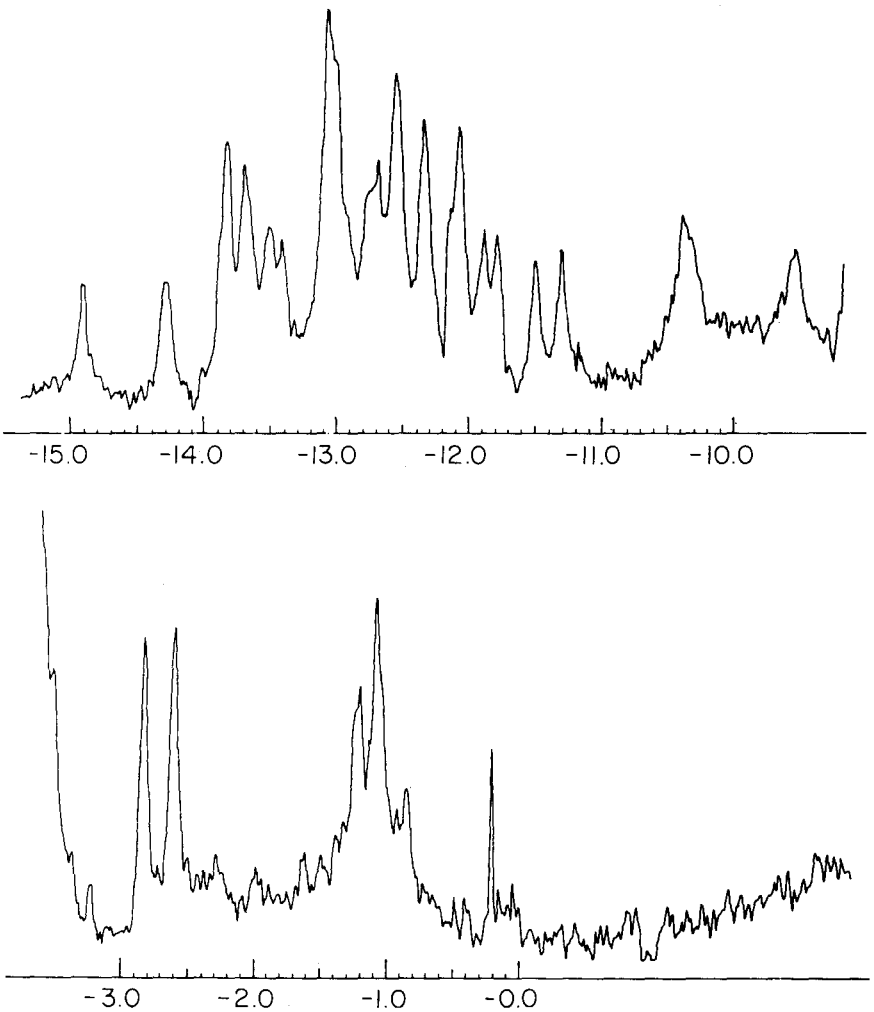

Fig. 2 Low field hydrogen bond and high methyl spectra of *E. coli* $tRNA_1^{Val}$ samples at identical concentrations. Duplicate samples (26.2 mg ml^{-1}) were prepared as described in the text in D_2O containing 15 mM $MgCl_2$, 0.1 M NaCl (lower spectrum) and in 10 mM cacodylate, 15 mM $MgCl_2$, 0.1 M NaCl, 1 mM EDTA, *p*H 7.0, H_2O buffer (upper spectrum). Both spectra were accumulated at the same r.f. power for 1.500 sweeps of 16 s each at a temperature of 38 °C.

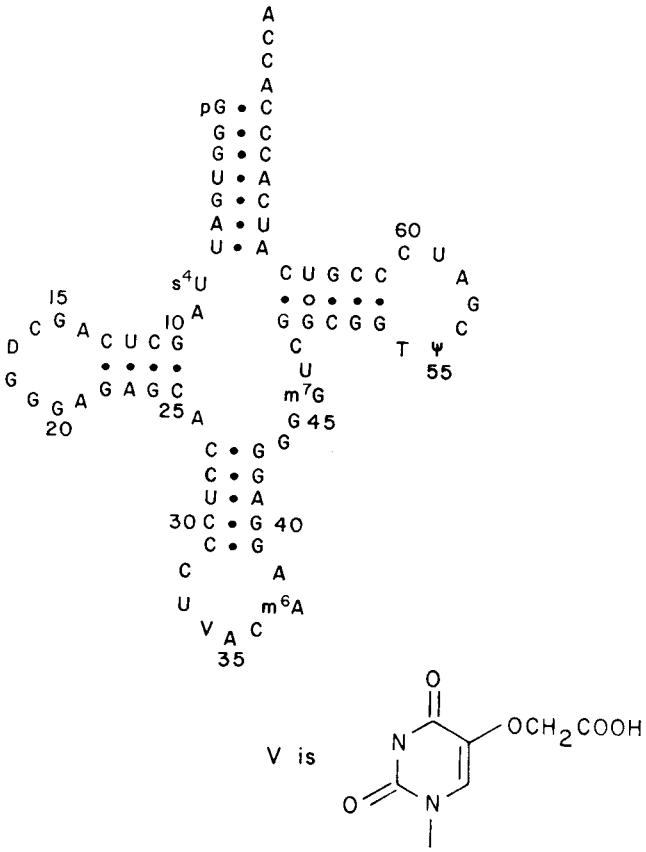

Fig. 3 The cloverleaf structure of *E. coli* $tRNA_1^{Val}$ as reported by Yaniv and Barrell[23] and by Kimura *et al.*[24].

Expected chemical shifts for tertiary resonances

The environment of the various tertiary base pairs in the crystal structure, together with the approximate ring current shift contributions from neighbouring bases determined previously[5], can now be used to estimate the approximate position of these tertiary resonances. The s^4U8–A14 tertiary interaction has been assigned to peak A at −14.9 p.p.m. by chemical modification with cyanogen bromide[15]; additional modifications of this unique sulphur in *E. coli* $tRNA_1^{Val}$ and *E. coli* $tRNA^{Arg}$ by Wong *et al.*[21] agree with this assignment. The reason for the extreme low field position of this tertiary resonance is the inherently greater deshielding of the ring NH of s^4U compared with U.

The T54–A58 interaction involves a ring NH · · · ring N bond. It is stacked with G18–ψ55 on one side and with G53–C61 on the other side; hence this resonance will be only moderately upfield shifted by neighbouring ring current effects. Since AT pairs have similar resonance positions to AU pairs[22], we would expect the T54–A58 resonance to be somewhere in the −13.5 to −14 p.p.m. region, that is peaks C, D, E or F (peak B is in the position expected for the secondary AU6 pair).

The G19–C56 interaction is a standard Watson–Crick pair with a ring NH · · · ring N bond. This tertiary pair is interesting in that it constitutes one extremity of the molecule with no residue on one side and G57 stacked on the other side. Thus, this resonance would be only moderately shifted from −13.6 p.p.m. to somewhere in the −12.7 to −13.3 p.p.m. range, that is peak G, H or I.

The m^7G46 to G22 tertiary interaction is a ring NH bond from m^7G46 to the ring N of G22. Its environment involves stacking with A21, A14, A9 and A23[19]. Since adenine is the most potent ring current shift base[5], this resonance would suffer an extremely large upfield shift—perhaps 2 p.p.m. or more. Thus the 46–22 tertiary resonance would be expected in the −11 to −12 p.p.m. region (peak M, N, O or P).

The 15–48 and 18–55 tertiary interactions involve ring NH protons which do not bond to ring nitrogens but instead bond to oxygen atoms. Such bonding has been shown to be less deshielding[1] and in addition these bonds would suffer an average upfield ring current shift from their stacking neighbours[19]. Thus the 15–48 and 18–55 resonances would be expected at the high field end of the spectrum between −11 and −12 p.p.m., that is peak M, N, O or P.

To summarise, the 8–14 interaction is at −14.9 p.p.m. and the 54–58 and 19–56 interactions are probably around −13.7 p.p.m. and around −13.0 p.p.m. respectively. The crystallographic data also lead us to predict that the three remaining tertiary resonances—15–48, 18–55 and 46–22—will all be in the −11 to −12 p.p.m. region; the spectrum reveals four protons in this region and the secondary pair G5–C68 is predicted to be at −11.6 p.p.m.

Tertiary structure in absence of magnesium

The low spectrum in Fig. 1 is that of a sample dialysed for 48 h against three changes (6 l each) of double distilled water, lyophilised, and then dissolved in 10 mM sodium cacodylate, 10 mM sodium-EDTA, *p*H 7.0, at a concentration of 1 mM tRNA. The sodium ion concentration in the

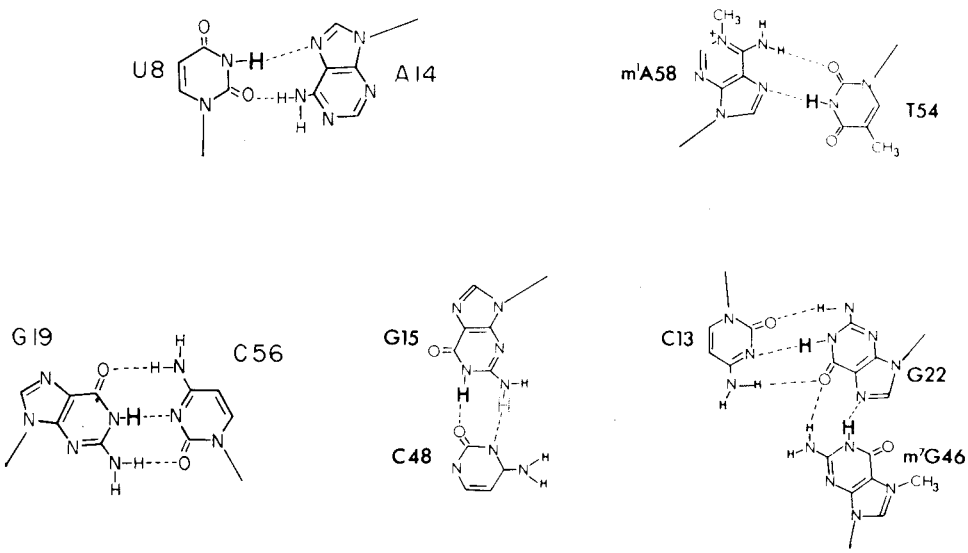

Fig. 4 Tertiary hydrogen bonding interactions seen in the crystal structure of yeast $tRNA^{Phe}$ determined by Kim *et al.*[17,19] and by Robertus *et al.*[18] and Klug *et al.*[20]. Only interactions involving ring NH hydrogen bonds are shown and these are denoted in bold face.

added solvent is 40±5 mM. The lyophilised tRNA is the sodium salt and, at 1 mM, would generate another 75±5 mM sodium ion. This excess EDTA-no magnesium solvent was chosen in the hope of destabilising tRNA tertiary structure. The 35 °C (and also the 45 °C) spectrum revealed, however, that all 26 resonances are still present. There are only two resonances which shift slightly in the non-magnesium structure; peak E (−13.5 p.p.m.) shifts downfield slightly into peak D, and peak I (−12.7 p.p.m.) shifts upfield slightly into peak J. Although it is difficult to interpret unambiguously such a subtle change, our current hypothesis is that the stacking of the acceptor helix on the rT helix (base pair 7 on base pair 49) is changed from the imperfect 17° stack[17] to a more colinear stack. Concomitant with this change is a noticeable sharpening of the resonance at −10.4 p.p.m. We have assigned this resonance to the secondary G50–U64 pair[15] which is presumably more protected from solvent exchange in the new structure.

The major conclusion to be drawn from these two spectra, however, is that all the tertiary interactions are formed even in the absence of magnesium; in fact the lack of spectral changes in all the other resonances suggests that the non-magnesium structure is remarkably similar to the magnesium-stabilised structure. Stabilisation of the structure by traces of residual bound magnesium can be discounted since heating the 1 mM tRNA sample in 10 mM EDTA to 65 °C for 1 h followed by subsequent cooling to 35 °C, resulted in a spectrum identical to the lower spectrum in Fig. 1.

Relation to earlier tRNA NMR data

We have now shown that *E. coli* $tRNA_1^{Val}$, with 20 secondary base pairs, contains six tertiary base pair resonances in its low field NMR spectrum; do the other class 1 tRNAs studied previously really have no tertiary resonances as claimed, or have their spectra been misinterpreted? The spectrum of yeast $tRNA^{Phe}$ has been studied in greatest detail and has assumed the role of a 'reference spectrum'[2–6,8–12]. The integration of low field spectra has been complicated by the lack of suitable internal standards with such large chemical shifts. Using Met-cyanomyoglobin as an external standard Wong *et al.*[4], after normalising the two spectra to the same molar concentrations and the same number of accumulated sweeps, arrived at an intensity of 18.6 protons in the total spectrum. A composite peak at −13.7 p.p.m. was found to contain slightly more than three protons; this peak was normalised to 3.00 protons and subsequently became an 'internal standard'. A more recent revision by Kearns *et al.*[10] reported a value of 19.7 protons for the total intensity of the yeast $tRNA^{Phe}$ spectrum, but again made the assumption that the −13.7 p.p.m. peak contained three protons. We have re-examined the low field spectrum of yeast $tRNA^{Phe}$ at 360 MHz (manuscript in preparation). At this resolution the peak at −13.7 p.p.m. resolves into three peaks of intensity 1:2:1, that is it contains four protons. Since this peak has previously been assumed to contain three protons and was used as an internal standard, it follows that the true intensity should be 1.33 times higher than reported. We note that 1.33 times 19.7 is in fact very close to 26. Independent integration of the yeast $tRNA^{Phe}$ 360-MHz spectrum, which resolves into 14 peaks instead of the nine peaks in the 300-MHz spectrum, leads to a value of 26±1 protons. Thus, we believe that all class I tRNAs probably contain approximately six tertiary resonances in their low field spectra, and previous NMR analyses have been erroneously interpreted.

We thank Susan Ribeiro and Lillian McCollum for technical assistance. This work was supported by grants from the US Public Health Service and the US National Science Foundation to B.R.R.. The use of the Dutch NMR facility at the University of Groningen and the support of the Netherlands ZWO is acknowledged.

Received June 9; accepted August 6, 1975.

1 Katz, L., and Penman, S., *J. molec. Biol.*, **15**, 220–231 (1966).
2 Kearns, D. R., Patel, D., and Shulman, R. G., *Nature*, **229**, 338–339 (1971).
3 Kearns, D. R., Patel, D., Shulman, R. G., and Yamane, T., *J. molec. Biol.*, **61**, 265–270 (1971).
4 Wong, Y. P., Kearns, D. R., Reid, B. R., and Shulman, R. G., *J. molec. Biol.*, **72**, 725–740 (1972).
5 Shulman, R. G., Hilbers, C. W., Kearns, D. R., Reid, B. R., and Wong, Y. P., *J. molec. Biol.*, **78**, 57–69 (1973).
6 Lightfoot, D. R., Wong, K. L., Kearns, D. R., Reid, B. R., and Shulman, R. G., *J. molec. Biol.*, **78**, 71–89 (1973).
7 Shulman, R. G., *et al.*, *Proc. natn. Acad. Sci. U.S.A.*, **70**, 2042–2045, (1973).
8 Wong, Y. P., Reid, B. R., and Kearns, D. R., *Proc. natn. Acad. Sci. U.S.A.*, **70**, 2193–2195 (1973).
9 Kearns, D. R., *et al.*, *Ann. N.Y. Acad. Sci.*, **222**, 324–336 (1973).
10 Kearns, D. R., Wong, K. L., and Wong, Y. P., *Proc. natn. Acad. Sci. U.S.A.*, **70**, 3843–3846 (1973).
11 Hilbers, C. W., Shulman, R. G., and Kim, S. H., *Biochem. biophys. Res. Commun.*, **55**, 953–960 (1973).
12 Jones, C. R., and Kearns, D. R., *Proc. natn. Acad. Sci. U.S.A.*, **71**, 4237–4240 (1974).
13 Kearns, D. R., and Shulman, R. G., *Accounts Chem. Res.*, **7**, 33 (1974).
14 Crothers, D. M., Cole, P. E., Hilbers, C. W., and Shulman, R. G., *J. molec. Biol.*, **87**, 63–88 (1974).
15 Reid, B. R., *et al.*, *Proc. natn. Acad. Sci. U.S.A.*, **72**, 2049–2053 (1975).
16 Kan, L. S., T'so, P. O. P., Haar, F.v.d., Sprinzl, M., and Cramer, F., *Biochem. biophys. Res. Commun.*, **59**, 22–29 (1974).
17 Kim, S. H., *et al.*, *Science*, **185**, 435–440 (1974).
18 Robertus, J. D., *et al.*, *Nature*, **250**, 546–551 (1974).
19 Kim, S. H., *et al.*, *Proc. natn. Acad. Sci. U.S.A.*, **71**, 4970–4974 (1974).
20 Klug, A., Ladner, J., and Robertus, J. D., *J. molec. Biol.*, **89**, 511–516 (1974).
21 Wong, K. L., Bolton, P. H., and Kearns, D. R., *Biochim. biophys. Acta*, **383**, 446–451 (1975).
22 Crothers, D. M., Hilbers, C. W., and Shulman, R. G., *Proc. natn. Acad. Sci. U.S.A.*, **70**, 2899–2901 (1973).
23 Yaniv, M., and Barrell, B. G., *Nature*, **222**, 278–279 (1969).
24 Kimura, F., Harada, F., and Nishimura, S., *Biochemistry*, **10**, 3277–3283 (1971).

letters to nature

X-ray outburst from the direction of the galactic centre

WHEN the Uhuru satellite examined the X-ray emission from the region of the galactic centre in 1971 an extended region of emission centred on the radio source Sgr A and about 2° in extent was observed[1]. We report here details of a transient point X-ray source, A1742−28, which has been observed at the centre of this region by the Ariel V rotation modulation collimator (RMC) experiment. Its rise to a peak and subsequent decline by a factor of two over 12 d were monitored. The position was found to be $\alpha = 17\,h\ 42\,min\ 26.0 \pm 4.8\,s$, $\delta = -28°\ 59.8 \pm 1.2'$ (1950.0 coordinates, 90% confidence limits).

Figure 1 shows the intensity variation of the new source. Observations were made primarily in the photon energy range 3.0 to 7.5 keV although some data were obtained in the range 4.6–12 keV. Each plotted point represents observations spread over a period of one orbit (101 min). The RMC experiment is primarily designed to measure positions of point sources and has a grid pitch to separation ratio of 112, corresponding to an image response with full width at half maximum (FWHM) of